**L39**

# HIGH RESOLUTION POWDER DIFFRACTION

## A.N. Fitch

*ESRF, BP220, 38043 Grenoble Cedex, France*

*Keywords: powder diffraction, high resolution, beamline, peak shape*

*e-mail: fitch@esrf.fr*

High resolution powder X-ray diffraction beam lines operate at many synchrotron radiation sources, exploiting the very high intensity, vertical collimation and wavelength tunability of the beam. At ESRF in Grenoble, a powder diffraction beam line has operated since May 1996. Originally built on the BM16 bending magnet source [1], the diffractometer was transferred six years ago to a new location at ID31, where it is powered by three 11-mm minimum gap undulators, to give very intense beams in the operational range of 6 keV – 60 keV (wavelength $\approx$2 Å – 0.2 Å). The diffractometer, shown in Figure 1, is equipped with a bank of post-sample analyser crystals, Figure 2, to give very high angular resolution as well as accuracy. An analyser crystal, rather than inferring the $2\theta$ angle of diffraction from the position of a slit or pixel on a PSD, defines a true angle of diffraction, and thereby removes a number of systematic aberrations in the peak positions that affect standard configurations.
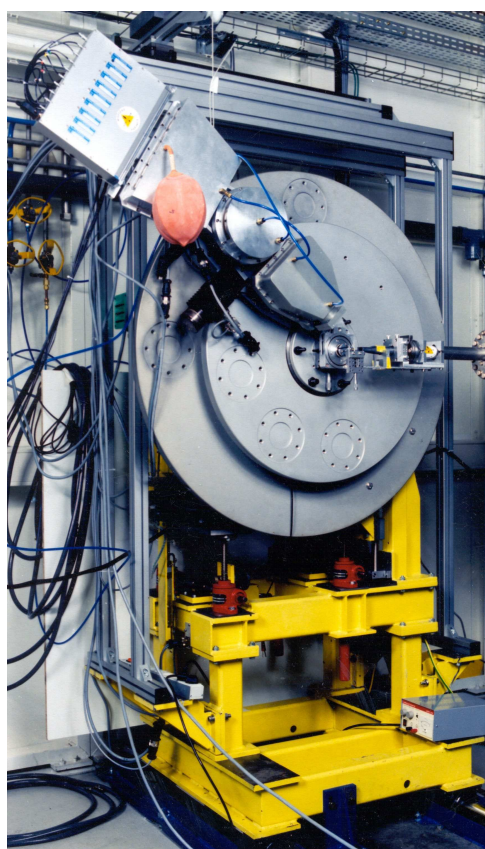


Figure 1. ID31's high resolution powder diffractometer, equipped with the nine crystal multianalyser stage.
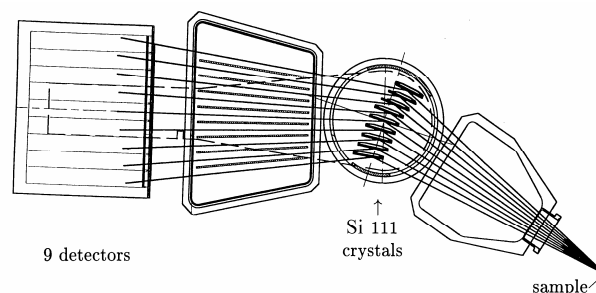


Figure 2. Nine channel Si 111 multianalyser stage [2]. Each channel is offset from the next by $\approx$2°. As the detector arm is scanned, nine high resolution powder diffraction patterns are collected in parallel, and these are subsequently combined and normalised in a data reduction step [3].

A wide range of sample environments is available, allowing measurements at temperatures from 3 K to 1600°C, and under a variety of atmospheres. A robotic sample changer permits up to 50 samples to be processed automatically. Typical uses of the beam line include;

- Structural studies: the solving and refining of crystal structures, exploration of the structure of glasses, and atomic pair distribution function (PDF) analysis;
- *In-situ* studies: observation of structures or materials evolving with temperature, time, voltage, etc. during phase transitions, solid-state chemistry, electrochemistry, *etc.*;
- Anomalous scattering: tuning to an absorption edge to help distinguish between elements with similar atomic number in a material;
- High throughput studies: involving many samples synthesised with different compositions, or under varied preparation conditions, *etc.*;
- Quantitative analysis: diffraction patterns from complex mixtures with many contributing phases can be analysed; the detection of phases present in very low proportions is possible;
- Microstructure: analysis of peak shapes yields microstructural information about a material. Since the instrumental contribution is very small, the peak shapes are dominated by sample effects;
- Residual strain: Measurements of residual strain, either by the traditional $sin^2\psi$ technique, or by mapping peak positions from within the bulk and surface of a sample, *etc.*;

- Diffraction at grazing incidence and reflectivity: measurements from thin films and surfaces.

The accessibility of high $2\theta$ resolution at short wavelengths is a particular strength of the beam line. Thus a wide range of absorbing materials can be investigated using spinning-capillary sample geometry. The use of a spinning capillary can greatly reduce preferred orientation effects, which are hard to avoid when using a flat-plate powder specimen, thus improving the accuracy of the measured diffraction intensities. Hard energies, 30 keV and above, also allow measurements to high values of $Q = 4\pi \sin\theta / \lambda$ for investigation of the atomic pair distribution function $G(r)$ of a material. The PDF is obtained by Fourier transforming the normalised scattered X-ray intensity and is a measure of the number of atoms in a spherical shell of radius $r$ about a reference atom. Thus peaks in $G(r)$ represent characteristic distances between pairs of atoms in the structure, and the method can be applied to crystalline and non-crystalline samples alike [4]. This allows structural characterisation of poorly crystalline and disordered materials that lack the translational periodicity of a good crystal. The analyser crystals help the quality of the PDF analysis by suppressing background contributions to the diffraction pattern coming from fluorescence and Compton scattering [5]. However scanning the analyser crystals requires several hours to collect data of sufficient statistical quality, and it is often advantageous to use a lower resolution arrangement with very hard X-rays (90 keV) and a two dimensional detector to record the whole scattering pattern in a single exposure [6], which may be a matter of less than a second. This approach is extensively used at the APS (Argonne National Laboratory).

In the development of new materials, analysis of the diffraction peak shapes can yield important chemical or microstructural information. For example, in the search for new hydrogen storage materials, cycling hydrogen between lithium nitride $Li_3N$, lithium imide $Li_2NH$, lithium amide $LiNH_2$ has been investigated [7]. Three samples that had undergone various cycles of hydrogen adsorption and desorption were examined on ID31. As well as a complex mixture of phases identified in sample I, including the unexpected new phase $Li_{1.15}NH_{1.85}$ (composition from the refined Li occupancy), some remarkable peak shapes were apparent in samples II and III, Figure 3, implying complex microstructural behaviour. The broad Bragg peaks of the dominant cubic Li-N-H phase are highly structured and follow a strain-broadening dependence on diffraction angle, indicative of a pronounced variation in stoichiometry. Detailed analysis of the pattern using the remarkable Rietveld refinement program TOPAS [8] allowed the range of non-stoichiometry to be evaluated. The peak shape was modelled as a sum of 11 phases, $Li_{1+x_n}NH_{2-x_n}$, with uniformly varying stoichiometry ($x_n$) and lattice parameter ($a_n$), refining the stoichiometric and lattice-parameter limits, $x_0$, $x_{10}$, $a_0$, $a_{10}$, and the amount of each phase present. Thus the compositional variation

represented by the complex peak profile can be obtained, which allowed a mechanism for hydrogen storage and release to be proposed.
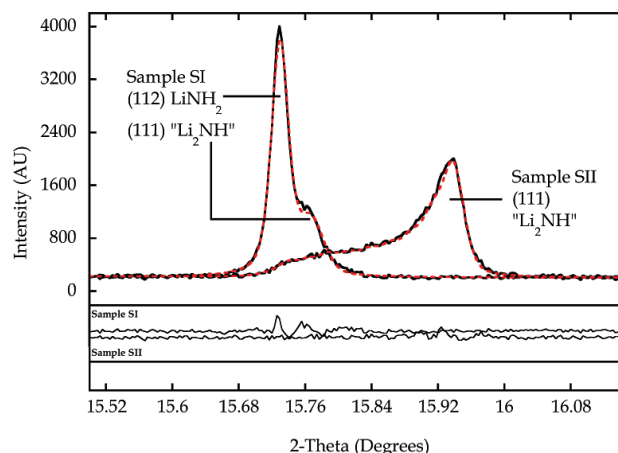


Figure 3. Some of the remarkable powder diffraction peak shapes seen from samples produced by hydrogen cycling in the lithium nitride-imide-amide system, and the fit using the Rietveld refinement program TOPAS, from Ref. [7].

With very high $2\theta$ resolution, the question arises as to just how big a structure can be analysed from a powder diffraction pattern, and measurements with protein samples have been pioneered by Von Dreele working at the NSLS (Brookhaven) [9, 10] and APS [11]. One of the bottlenecks in protein structure analysis is growing a suitable single crystal and modern screening approaches often produce polycrystalline material instead. Protein structures can be refined by the Rietveld method employing extensive stereochemical restraints to preserve the molecular structure, and even solved by molecular replacement *e.g.* for a variant of the $T_3R_3$ human insulin-zinc complex produced by grinding [10].

Remarkable progress has been made in the field, reviewed by Margiolaki and Wright [12]. Recently reported was the solution by molecular replacement of the structure of the second SH3 domain of the muscle protein Ponsin, with 67 amino acids in the chain, via a model with only 38% amino-acid sequence homology [13]. The analysis exploited multiple data sets with radiation-induced anisotropic shifts in peak positions to improve the amount of structural information that could be extracted from the powder data. Anisotropic peak shifts mean that peaks overlapping in one pattern may be better (or differently) resolved in another. By fitting simultaneously to the multiple data sets, the deleterious effects of peak overlap can be alleviated, to some extent at least. Anisotropic shifts in peak positions, reflecting underlying lattice strains, can be induced via changes in temperature [14], or for proteins via crystallisation at different pH values [15], with different solvents, or as a result of radiation damage in the very intense synchrotron X-ray beam [11, 13].
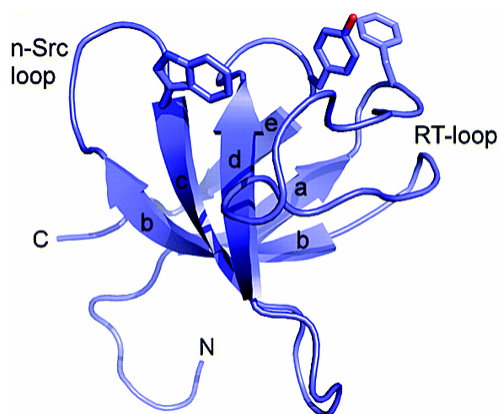
*ISSRNS 2008 – abstracts*

**L39**



Figure 4. Ribbon representation of the structure of the second SH3 domain of Ponsin determined by high resolution powder diffraction [13].

## References

[1] A.N. Fitch, "The high resolution powder diffraction beam line at ESRF", *J. Res. Natl. Inst. Stand. Technol.* **109** (2004) 133-142.

[2] J.-L. Hodeau, P. Bordet, M. Anne, A. Prat, A.N. Fitch, E Dooryhée, G. Vaughan, A. Freund, "Nine crystal multi-analyser stage for high resolution powder diffraction between 6 and 40 keV", *Proc. SPIE* **3448** (1998) 353-361.

[3] J.P. Wright, G.B.M. Vaughan, A.N. Fitch, "Merging data from a multi-detector continuous scanning powder diffraction system", *IUCr Computing Commission Newsletter* **1** (2003) 92-96, (http://www.iucr.org/iucr-top/comm/ccom/newsletters/2003jan/index.html).

[4] M.G. Kanatzidis, S.J.L. Billinge, "Beyond crystallography: the study of disorder, nanocrystallinity and crystallographically challenged materials with pair distribution functions", *Chem. Commun.* (2004) 749-760.

[5] S. Brühne, E. Uhrig, K.-D. Luther, W. Assmus, M. Brunelli, A.S. Masadeh, S.J.L. Billinge, "PDF from X-ray powder diffraction for nanometer-scale atomic structure analysis of quasicrystalline alloys", *Z. Krist*. **220** (2005) 962-967.

[6] P.J. Chupas, K.W. Chapman, P.L. Lee, "Applications of an amorphous silicon-based area detector for high-resolution, high-sensitivity and fast time-resolved pair distribution function measurements", *J. Appl. Crystallogr.* **40** (2007) 463-470.

[7] W.I.F. David, M.O. Jones, D.H. Gregory, C.M. Jewell, S.R. Johnson, A. Walton, P.P. Edwards, "A mechanism for non-stoichiometry in the lithium amide lithium imide hydrogen storage reaction", *J. Am. Chem. Soc.* **129** (2007) 1594-1601.

[8] A. Coelho, TOPAS Academic, see http://members.optusnet.com.au/alancoelho/.

[9] R.B. Von Dreele, "Combined Rietveld and stereochemical restraint refinement of a protein crystal structure", *J. Appl. Crystallogr.* **32** (1999) 1084-1089.

[10] R.B. Von Dreele, P.W. Stephens, G.D. Smith, R.H. Blessing, " The first protein crystal structure determined from high-resolution X-ray powder diffraction data: a variant of $T_3R_3$ human insulin-zinc complex produced by grinding", *Acta Crystallogr. D* **56** (2000) 1549-1553.

[11] R.B. Von Dreele, "Multipattern Rietveld refinement of protein powder data: an approach to higher resolution", *J. Appl. Crystallogr.* **40** (2007) 133-143.

[12] I. Margiolaki, J.P. Wright, " Powder crystallography on macromolecules", *Acta Crystallogr. A* **64** (2008) 169-180.

[13] I. Margiolaki, J.P. Wright, M. Wilmanns, A.N. Fitch, N. Pinotsis, "Second SH3 domain of ponsin solved from powder diffraction", *J. Am. Chem. Soc.* **129** (2007) 11865-11871.

[14] K. Shankland, W.I.F. David, D.S. Sivia, "Routine *ab initio* structure determination of chlorothiazide by X-ray powder diffraction using optimised data collection and analysis strategies", *J. Mater. Chem.* **7** (1997) 569-572.

[15] S. Basso, A.N. Fitch, G.C. Fox, I. Margiolaki, J.P. Wright, "High-throughput phase-diagram mapping *via* powder diffraction: A case study of HEWL *versus* pH", *Acta Crystallogr. D* **61** (2005) 1612-1625.